Catalysis Communications 124 (2019) 67–70

Contents lists available at ScienceDirect

Catalysis Communications

journal homepage: www.elsevier.com/locate/catcom

Short communication

Synthesis of nickel phosphide nanorods for hydrotreating reactions

Yu Zhao[a,*], Shidong Wang[a], Ning Li[a], Qi Zhang[a], Guixian Li[a], Jianyi Shen[b]

[a] School of Petrochemical Engineering, Lanzhou University of Technology, Lanzhou 730050, Gansu, China
[b] School of Chemistry and Chemical Engineering, Nanjing University, Nanjing 210093, Jiangsu, China

ARTICLE INFO

Keywords:
Nickel phosphate nanofibers
Ionothermal synthesis
Ni_2P nanorods
Hydrotreating reactions

ABSTRACT

Nickel phosphate (NiPO) nanofibers with high surface area (288 m^2/g) were obtained from phosphoric acid and nickel nitrate in an ionic liquid ([Bmim]Br) via an ionothermal synthesis process at 150 °C. Heating the nanofibers under a H_2 atmosphere at 700 °C led to the formation of Ni_2P nanorods, ~50 nm in diameter and 100–200 nm in length. The Ni_2P nanorod catalyst exhibited a much higher turnover frequency in the hydrodesulfurization of dibenzothiophene than the previously reported Ni_2P catalysts with nanoparticle, nanosheet or irregular block morphologies, which may be attributable to the morphology effect of the nanorods.

1. Introduction

Metal phosphide catalysts (e.g., Ni_2P) have received a lot of attention due to their high activity in hydrodesulfurization (HDS) and hydrodenitrogenation (HDN) reactions when compared to traditional Co (Ni)-Mo-S catalysts [1], and their increased thermal stability in a variety of sulfur-containing environments [2]. The latest report shows that Ni_2P is not only used as an excellent HDS catalyst, but also has extended application in other important reactions, such as the dehydrogenation [3] and hydrodeoxygenation reactions [4–6]. In addition, Ni_2P has been extensively studied as an electrode material in recent years [7,8], which shows its wide application prospects.

There have been many studies reporting various methods used to prepare Ni_2P, such as the temperature programmed reduction (TPR) of a range of nickel precursors and phosphorous sources in flowing H_2 at high temperature [9], phosphorization of nickel or nickel oxides using PH_3 [10], treatment of nickel in trioctylphosphine (TOP) [11], the self-oxidation-reduction reaction between nickel cations and hypophosphite or phosphite at low temperature [12,13], etc. Among these methods, the TPR method is the easiest and most stable, and thus, the most widely used. However, the high temperatures used in the TPR process may lead to the agglomeration and sintering of the Ni_2P particles, which results in bulk crystals. Ni_2P crystals with specific morphology are difficult to obtain using this method and has been rarely reported to date.

The synthesis of inorganic nanomaterials in ionic liquids has attracted a lot of attention since Morris et al. defined the term "ionothermal synthesis" in 2004 and prepared aluminophosphate zeolite analogues in ionic liquids or eutectic mixtures [14]. In this method, the ionic liquid acts as both the solvent and template, which makes the resulting mixture simpler. Ionic liquids have negligible vapor pressure, so the synthesis process can be carried out using an open system, which eliminates the danger of high pressures and makes the process easier. Many metal phosphates nanomaterials have been prepared using ionic liquids as solvent, such as aluminophosphate zeolite [15], zirconium phosphate [16], germanium phosphate [17] and vanadium phosphate catalysts [18]. However, the synthesis of nickel phosphate with special morphology using an ionothermal method has rarely been reported.

In this study, nickel phosphate nanofibers with high surface area were prepared using an ionothermal process. Hydrotreatment of this nanofiber precursor using the TPR method led to the formation of a Ni_2P catalyst with nanorod morphology. The Ni_2P nanorod catalyst was used in the HDS of dibenzothiophene (DBT) and hydrogenation of tetralin in a model diesel sample, which displayed higher catalytic activity than that of the corresponding Ni_2P nanosheet and nanoparticle catalysts, which was attributed to the morphology effect.

2. Experimental

2.1. Catalyst preparation

The [Bmim]Br ionic liquid was prepared according to a previous process [15]. The nickel phosphate nanofibers were prepared using an ionothermal method. A total of 2.91 g (0.01 mol) of $Ni(NO_3)_2{\cdot}6H_2O$ and 1.73 g (0.015 mol) of 85% phosphoric acid were added to 87.7 g (0.4 mol) of the as-prepared [Bmim]Br with constant stirring. The mixture was stirred at 50 °C for a period of time to ensure sufficient dissolution had occurred. The resulting solution was then heated to

* Corresponding author.
E-mail address: yzhao@lut.edu.cn (Y. Zhao).

https://doi.org/10.1016/j.catcom.2019.03.006
Received 24 October 2018; Received in revised form 25 February 2019; Accepted 5 March 2019
Available online 06 March 2019
1566-7367/

150 °C and heated at reflux for 72 h and then allowed to cool to room temperature. The resulting precipitate was filtered, washed three times with deionized water and two times with n-butyl alcohol, and dried at 120 °C for 12 h to give the nickel phosphate nanofibers (NiPO-IL) as a green solid.

To obtain the Ni_2P nanorods, a TPR step was carried out. The NiPO-IL precursor was heated under an atmosphere of flowing H_2 (40 mL/min) to 400 °C at a heating rate of 5 °C/min and then to 700 °C at a heating rate of 1 °C/min and finally kept at 700 °C for 2 h. After being cooled down to room temperature under an H_2 atmosphere, the material was passivated in 0.5% O_2/N_2 for 12 h. The resulting sample was named Ni_2P-IL.

For comparison, a nickel phosphate sample was also prepared via a traditional co-precipitation method using water as the reaction solvent, which was named NiPO-H_2O. The NiPO-H_2O precursor was then subjected to the TPR process under the same reaction conditions described above to prepare the Ni_2P sample, which was signed as Ni_2P-H_2O.

2.2. Characterization

The samples were characterized by N_2 adsorption-desorption measurements, X-ray diffraction (XRD), the microcalorimetric adsorption of CO, scanning electron microscopy (SEM). Experimental details can be seen in the supplementary information.

2.3. Catalytic tests

The catalytic tests were carried out for the HDS of DBT and hydrogenation of tetralin in a model diesel sample containing 1.72% DBT (3000 ppm S), 5% tetralin and 0.5% n-octane (as an internal standard) in n-nonane (solvent). A fixed-bed reactor was used to perform the reactions. The reaction conditions can be seen in the supplementary information.

3. Results and discussion

3.1. Textural and structural properties

Nickel phosphate nanofibers can be obtained via an ionothermal synthesis process using $Ni(NO_3)_2{\cdot}6H_2O$ and phosphoric acid in [Bmim]Br. Fig. 1(a) shows the SEM images of the final NiPO-IL material. It can be seen that the NiPO-IL sample exhibited a uniform nanofiber morphology with diameters in the range of 10–20 nm and several hundred nm in length. The reduction of this nanofiber precursor under a H_2 atmosphere at 700 °C led to the formation of the Ni_2P nanorod catalyst, 100–200 nm in length and 30–50 nm in diameter, as shown in Fig. 1(b). For comparison, the nickel phosphate sample prepared using a traditional co-precipitation method in water possessed an irregular block morphology (not shown). Thus, the ionic liquid played an important role in the synthesis of nickel phosphate with nanofiber morphology due to both its solvent and template effect. Nickel phosphates with nanofiber or nanotube morphologies have also been reported in past reports. However, almost all these materials are prepared using hydrothermal methods under a high temperature and high pressure environment and require the addition of a template agent, which is obviously more complex and dangerous than the ionothermal method described in this paper. During the preparation of Ni_2P via the TPR method, the reported Ni_2P products showed an irregular block morphology due to the significant aggregation of the particles at high temperature (650–750 °C). However, a Ni_2P catalyst with a uniform nanorod morphology could be still obtained after the TPR treatment at 700 °C in this work due to the high stability of the NiPO nanofiber precursor.

Fig. 2 shows the XRD patterns of the as-prepared NiPO and those obtained after reduction in flowing H_2 at 400 °C and 700 °C, respectively. The nickel phosphate nanofibers prepared via an ionothermal

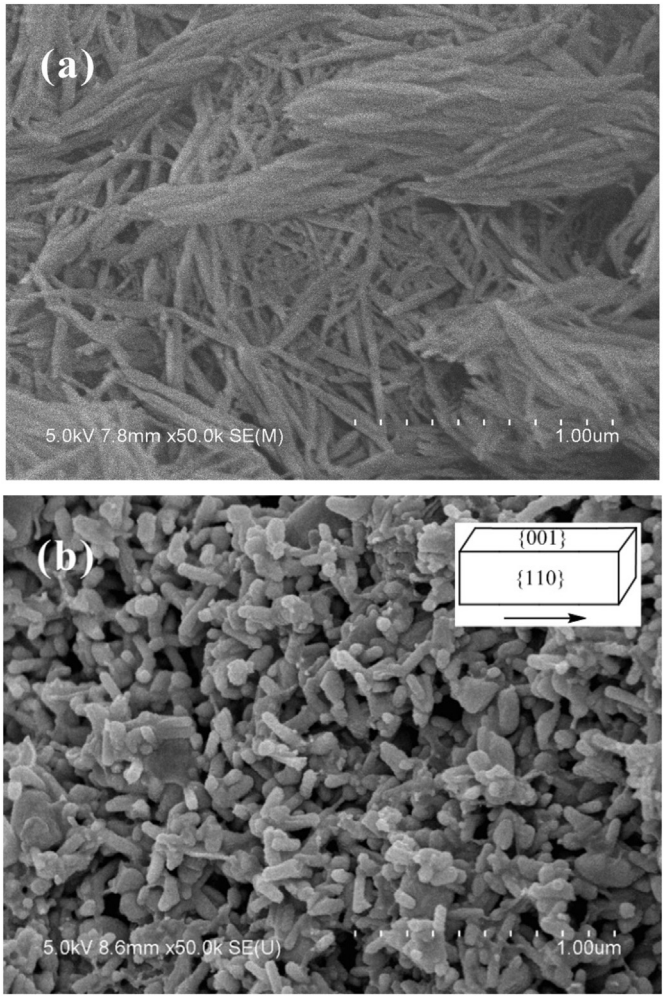

Fig. 1. SEM images of NiPO-IL (a) and Ni_2P-IL (b).

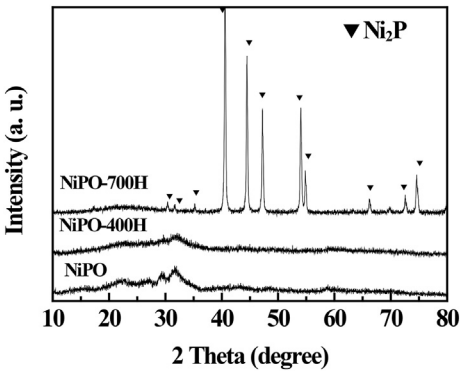

Fig. 2. XRD patterns of as-prepared NiPO and after reduction in flowing H_2 at 400 °C and 700 °C, respectively.

process exhibited a series of broad peaks in the range of 25–35°, indicating that it was prepared in a mainly amorphous phase. After treatment of this nanofiber precursor in H_2 at 400 °C, the XRD patterns of the product still showed a broad peak in the range of 25–35°, which showed the high stability of the NiPO-IL precursor. When the reduction temperature was increased to 700 °C, sharp diffraction peaks were detected, which were all consistent with crystalline Ni_2P (JCPDS No. 74–1385) indicating that a high-purity Ni_2P catalyst was prepared using the TPR process. According to Scherrer equation, the average sizes of Ni_2P crystallites were estimated to be about 33.7 nm which was

Table 1
Surface properties of the catalysts.

Samples	Surface area (m^2/g)	Pore volume (cm^3/g)	Average pore diameter (nm)
NiPO-IL	288	1.69	25.0
NiPO-H_2O	44	0.06	5.7
Ni_2P-IL	14	–	–
Ni_2P-H_2O	2	–	–

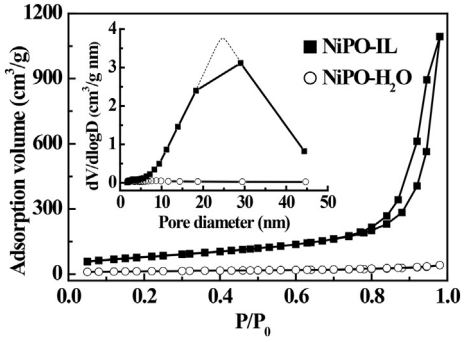

Fig. 3. N_2 adsorption-desorption isotherms of NiPO-IL and NiPO-H_2O. Inset shows the corresponding pore size distributions.

confirmed by SEM.

Table 1 summarizes the specific surface area, pore volume and pore diameter of the as-prepared samples. The nickel phosphate nanofibers (NiPO-IL) prepared via an ionothermal synthesis method possessed a high surface area of 288 m^2/g, while the surface area of the NiPO-H_2O sample prepared in water was only 44 m^2/g. The pore volume of NiPO-IL was 1.69 cm^3/g, while that of NiPO-H_2O was small. Fig. 3 shows the N_2 adsorption-desorption isotherms and pore size distribution curves obtained for the NiPO-IL and NiPO-H_2O samples. NiPO-H_2O only possessed a very low adsorption capacity and showed an extremely weak pore size distribution peak at ~6 nm. However, NiPO-IL exhibited a high adsorption capacity and the N_2 adsorption-desorption isotherms were typical of type IV with H3 model hysteresis loops, which indicated a mesoporous structure. The corresponding pore size distribution of NiPO-IL showed a relatively narrow peak at ~25 nm, which was probably from the fiber packing gaps.

After heat treatment of NiPO-IL under an H_2 atmosphere at 700 °C, the as-obtained Ni_2P-IL catalyst possessed a surface area of 14 m^2/g, which was significantly decreased when compared with the NiPO-IL precursor due to its deoxidation process and structural modification at high temperature. However, the surface area of the Ni_2P-IL catalyst was still much higher than that of Ni_2P-H_2O (2 m^2/g) prepared via the TPR process of NiPO-H_2O.

3.2. The surface properties as-probed by the microcalorimetric adsorption of CO

The adsorption of CO can be used to titrate the number of surface active sites in a Ni_2P catalyst [19]. Thus, the microcalorimetric adsorption of CO on the Ni_2P catalysts prepared in this work was carried out and the results were shown in Fig. 4. The Ni_2P/NiPO nanosheet catalyst (Eut-NP3-H) reported in our previous work [20] was prepared from the self oxidation-reduction reaction of nickel hypophosphite in the eutectic mixture and possessed an initial heat of 79 kJ/mol. The initial heats for the Ni_2P-IL sample prepared in this work was 74 kJ/mol, which was similar with that of Eut-NP3-H indicating a similar number of active sites are present on the surface of these Ni_2P catalysts. The saturation coverage of CO was measured to be about 38 and 19 μmol/g for the Eut-NP3-H nanosheet and Ni_2P-IL nanorod catalysts, respectively. Although the Ni_2P-IL catalyst possessed a lower number of

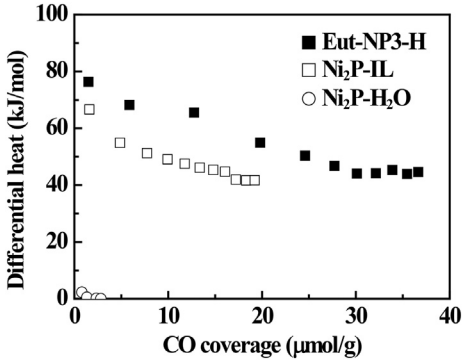

Fig. 4. Microcalorimetric adsorption of CO over the samples.

surface active sites on Ni_2P than the Eut-NP3-H catalyst, considering the surface area of the Eut-NP3-H sample was much higher than that of the Ni_2P-IL nanorod catalyst (133 m^2/g vs. 14 m^2/g), the adsorption quantity of CO per surface area observed for the Ni_2P-IL nanorod sample was much higher than that of the Eut-NP3-H sample, which was attributed to the morphology effect. For comparison, the Ni_2P-H_2O sample prepared in water possessed an extremely low adsorption quantity of CO (3 μmol/g) and small initial heat, indicating the low number of active sites in this sample due to its low surface area.

3.3. Catalytic behavior

The as-synthesized Ni_2P-IL nanorod catalyst and two other catalysts (Eut-NP3-H and Ni_2P-H_2O) were used for the HDS of DBT and the hydrogenation of tetralin in a model diesel sample. At 3.1 MPa, a weight hourly space velocity (WHSV) of 4 h^{-1} and 360 °C, the conversion of DBT was observed to be 60.2% and 75.8% on Ni_2P-IL and Eut-NP3-H, respectively, which was much higher than that observed on the Ni_2P-H_2O catalyst (44.8%). Two products (biphenyl and cyclohexylbenzene) were detected for the HDS of DBT over the catalysts in this work. The selectivity to cyclohexylbenzene and biphenyl was found to be about 15.2 and 84.8%, respectively, over the Ni_2P-IL at 360 °C, which was similar to that for the Eut-NP3-H (13.7 and 86.3%, respectively) [20], indicating that the reactions were all mainly through the direct desulfurization (DDS) mechanism over the two catalysts. Although the performance of Ni_2P-IL was lower than that of the Eut-NP3-H catalyst, a full comparison of the intrinsic activity over the two catalysts could not obtained from the numerical value of the conversions due to the great differences between the surface area of the two catalysts. Thus, the inherent HDS activity of the Ni_2P catalysts were calculated in the form of the turnover frequency (TOF) based on two standards, which was the number of active sites and surface area, respectively. The HDS TOF based on the number of active sites was calculated according to the equation $TOF_{activity\ sites} = QX/S$, where Q is the molar rate of DBT, X is the conversion and S is the number of moles of sites loaded (the mass of catalysts loaded multiplied by the adsorption quantity of CO). The value of $TOF_{activity\ sites}$ obtained for the Eut-NP3-H nanosheet catalyst was obtained to be 0.0021 s^{-1}, while that for Ni_2P-IL nanorod catalyst was 0.0033 s^{-1}. Obviously, the inherent HDS activity of the Ni_2P nanorod catalyst was higher than that of the nanosheet catalyst, which was also much higher than the other nanoparticle metal phosphide catalysts reported in the literature (such as Ni_2P/SiO_2 (0.0015 s^{-1}) [21] and CoP/γ-Al_2O_3 (0.00177 s^{-1}) [22]) as seen in Fig. 5. For the HDS TOF based on the surface area of the catalysts, it was also calculated according to the equation $TOF_{surface\ areas} = QX/S$, where Q is the molar rate of DBT, X is the conversion, while the substitutional S is the total surface area loaded (the mass of catalysts loaded by the BET specific surface area). The calculated value of $TOF_{surface\ areas}$ obtained for the Ni_2P-IL nanorod catalyst was 0.0045 mol·s^{-1}·m^{-2}, while that for the Eut-NP3-H nanosheet catalyst was only 0.00059 mol·s^{-1}·m^{-2}. The HDS

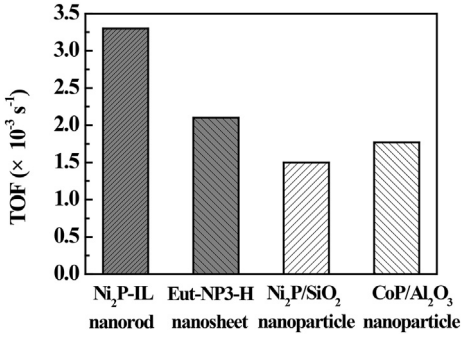

Fig. 5. The HDS TOF based on active sites over nanorod Ni_2P-IL catalyst and previous reported metal phosphide catalysts.

$TOF_{surface\ areas}$ for the Ni_2P nanorod catalyst was an order of magnitude higher than that observed for the nanosheet catalyst. Upon combining the two series of results mentioned above, the inherent HDS activity of the Ni_2P nanorod catalyst was higher than that of the nanosheet catalyst and the other irregular morphology catalysts probably due to the morphology effect [23].

The number of multi-ring hydrocarbons in diesel fuel is also an important parameter for fuel oil quality because they have low cetane numbers. In this work, tetralin was chosen as a model compound to study the catalytic hydrogenation of aromatic rings. At 360 °C, the conversion of tetralin over the Ni_2P-IL nanorod catalyst was about 8.2%, which was similar with that of the Eut-NP3-H nanosheet catalyst (8.9%), while that over the Ni_2P-H_2O catalyst was only 3.1% (see Fig. S1 in SI). In consideration of the great differences observed between the Ni_2P-IL and Eut-NP3-H catalyst, the Ni_2P-IL nanorod catalyst was superior over the Eut-NP3-H catalyst. Under the current reaction conditions, the hydrogenation of tetralin led to the formation of decalin while the dehydrogenation of tetralin produced naphthalene. Due to the cetane number of naphthalene being zero, the dehydrogenation of tetralin should be restrained. At 360 °C, the selectivity to decalin (total of *trans*- and *cis*-decalin) over the Ni_2P-IL nanorod catalyst reached 42.2%, which was much higher than that observed over the Eut-NP3-H (28.2%) and Ni_2P-H_2O (only 6.7%) catalysts, indicating the high hydrogenation activity of the Ni_2P-IL nanorod catalyst due to the morphology effect.

4. Conclusions

Phosphoric acid and nickel nitrate were heated at 150 °C in an ionic liquid ([Bmim]Br) resulting in the formation of nickel phosphate (NiPO) nanofibers with a high surface area of 288 m^2/g. Heating this material under an atmosphere of H_2 at 700 °C using a TPR process led to the formation of Ni_2P nanorods, ~50 nm diameter and 100–200 nm length. Ni_2P catalysts prepared with specific morphologies using a TPR method have been rarely reported because the high temperature used in the process often leads to agglomeration and sintering of the Ni_2P particles, which commonly results in an irregular block morphology. The hydrogenation activity over the as-synthesized Ni_2P nanorod catalyst was investigated using the HDS of DBT and hydrogenation of tetralin in a model diesel sample. Due to the morphology effect, the Ni_2P nanorods catalyst exhibited a much higher turnover frequency (TOF) in the HDS of DBT and hydrogenation of tetralin than the previous reported Ni_2P catalysts with nanoparticle, nanosheet or irregular block morphologies.

Acknowledgements

This work was supported by the National Natural Science Foundation of China (21203081 and 21763016) and Natural Science Foundation of Gansu Province (18YF1GA062 and 2017GS10924).

Appendix A. Supplementary data

Supplementary data to this article can be found online at https://doi.org/10.1016/j.catcom.2019.03.006.

References

[1] H. Song, Q. Yu, Y.G. Chen, Y.Y. Wang, R.X. Niu, Preparation of highly active MCM-41 supported Ni_2P catalysts and its dibenzothiophene HDS performance, Chin. J. Chem. Eng. 26 (2018) 540–544.
[2] Y.K. Lee, S.T. Oyama, Sulfur resistant nature of Ni_2P catalyst in deep hydrodesulfurization, Appl. Catal. A Gen. 548 (2017) 103–113.
[3] J.F. Li, Y.M. Chai, B. Liu, Y.L. Wu, X.H. Li, Z. Tang, Y.Q. Liu, C.G. Liu, Appl. Catal. A Gen. 469 (2014) 434–441.
[4] Y.X. Yang, C. Ochoa-Hernández, P. Pizarro, V.A.P. O'Shea, J.M. Coronado, D.P. Serrano, Influence of the Ni/P ratio and metal loading on the performance of Ni_xP_y/SBA-15 catalysts for the hydrodeoxygenation of methyl oleate, Fuel 144 (2015) 60–70.
[5] J.S. Moon, E.G. Kim, Y.K. Lee, Active sites of Ni_2P/SiO_2 catalyst for hydrodeoxygenation of guaiacol: a joint XAFS and DFT study, J. Catal. 311 (2014) 144–152.
[6] A. Iino, A. Takagaki, R. Kikuchi, S.T. Oyama, K.K. Bando, Combined in situ XAFS and FTIR study of the hydrodeoxygenation reaction of 2-Methyltetrahydrofuran on Ni_2P/SiO_2, J. Phys. Chem. C (2018), https://doi.org/10.1021/acs.jpcc.8b03246.
[7] R.B. Wexler, J.M.P. Martirez, A.M. Rappe, Chemical pressure-driven enhancement of the hydrogen evolving activity of Ni_2P from nonmetal surface doping interpreted via machine learning, J. Am. Chem. Soc. 140 (2018) 4678–4683.
[8] Y.J. Li, H.C. Zhang, M. Jiang, Q. Zhang, P.L. He, X.M. Sun, 3D self-supported Fe-doped Ni_2P nanosheet arrays as bifunctional catalysts for overall water splitting, Adv. Funct. Mater. 27 (2017) 1702513.
[9] S.J. Sawhill, D.C. Phillips, M.E. Bussell, Thiophene hydrodesulfurization over supported nickel phosphide catalysts, J. Catal. 215 (2003) 208–219.
[10] S.F. Yang, C.H. Liang, R. Prins, A novel approach to synthesizing highly active Ni_2P/SiO_2 hydrotreating catalysts, J. Catal. 237 (2006) 118–130.
[11] A.E. Henkes, Y. Vasquez, R.E. Schaak, Converting metals into phosphides: a general strategy for the synthesis of metal phosphide nanocrystals, J. Am. Chem. Soc. 129 (2007) 1896–1897.
[12] J.A. Cecilia, A. Infantes-Molina, E. Rodriguez-Castellon, A. Jimenez-Lopez, A novel method for preparing an active nickel phosphide catalyst for HDS of dibenzothiophene, J. Catal. 263 (2009) 4–15.
[13] G.J. Shi, J.Y. Shen, New synthesis method for nickel phosphide nanoparticles: solid phase reaction of nickel cations with hypophosphites, J. Mater. Chem. 19 (2009) 2295–2297.
[14] E.R. Cooper, C.D. Andrews, P.S. Wheatley, P.B. Webb, P. Wormald, R.E. Morris, Ionic liquids and eutectic mixtures as solvent and template in synthesis of zeolite analogues, Nature 430 (2004) 1012–1016.
[15] E.R. Parnham, R.E. Morris, 1-Alkyl-3-methyl imidazolium bromide ionic liquids in the ionothermal synthesis of aluminium phosphate molecular sieves, Chem. Mater. 18 (2006) 4882–4887.
[16] S. Smeets, L. Liu, J.X. Dong, L.B. McCusker, Ionothermal synthesis and structure of a new layered zirconium phosphate, Inorg. Chem. 54 (2015) 7953–7958.
[17] W. Wang, Y. Li, L. Liu, J.X. Dong, The first ionothermal synthesis of a germanium phosphate with one-dimensional chain-like structure, Dalton Trans. 41 (2012) 10511–10513.
[18] G.X. Li, Q. Zhang, W.G. Fang, Y. Zhao, Ionothermal synthesis and selective oxidation performance of a crystalline vanadium phosphate catalyst, Energy Environ. Focus 4 (2015) 301–306.
[19] Y. Zhao, M.W. Xue, M.H. Cao, J.Y. Shen, A highly loaded and dispersed Ni_2P/SiO_2 catalyst for the hydrotreating reactions, Appl. Catal. B Environ. 104 (2011) 229–233.
[20] Y. Zhao, Y.P. Zhao, H.S. Feng, J.Y. Shen, Synthesis of nickel phosphide nano-particles in a eutectic mixture for hydrotreating reactions, J. Mater. Chem. 21 (2011) 8137–8145.
[21] X.Q. Wang, P. Clark, S.T. Oyama, Synthesis, characterization, and hydrotreating activity of several iron group transition metal phosphides, J. Catal. 208 (2002) 321–331.
[22] J.A. Cecilia, A. Infantes-Molina, E. Rodríguez-Castellón, A. Jiménez-López, Dibenzothiophene hydrodesulfurization over cobalt phosphide catalysts prepared through a new synthetic approach: effect of the support, Appl. Catal. B Environ. 92 (2009) 100–113.
[23] D.V. Thuan, N.T. Khoa, S.W. Kim, E.J. Kim, S.H. Hahn, Morphology-dependent selective hydrogenation catalysis of hollow AuCu bimetallic nanostructures, J. Catal. 329 (2015) 144–150.